Available online at www.sciencedirect.com
ScienceDirect
Journal of Molecular Catalysis A: Chemical 265 (2007) 98–108
JOURNAL OF MOLECULAR CATALYSIS A: CHEMICAL
www.elsevier.com/locate/molcata

Pd complexes containing non-symmetrical diphosphines in the terpolymerization of ethene, propene and carbon monoxide

Antonella Leone [a], Sebastian Gischig [b], Giambattista Consiglio [a,*]

[a] *Eidgenössische Technische Hochschule, Institut für Chemie und Bioingenieurwissenschaften, Hönggerberg, Wolfgang-Pauli Strasse 10, CH-8093 Zürich, Switzerland*

[b] *Eidgenössische Technische Hochschule, Laboratorium für Anorganische Chemie, Hönggerberg, CH-8093 Zürich, Switzerland*

Received 25 April 2006; received in revised form 10 June 2006; accepted 28 September 2006
Available online 7 October 2006

Abstract

The preparation and the characterization of palladium(II) neutral dichloro complexes [$PdCl_2$(PˆP′)] **1a–d** and cationic disolvento complexes [Pd(PˆP′)$(H_2O)_2$](OTf)$_2$ **3a–d** containing non-symmetrical C_s-symmetrical diphosphines are reported.

Terpolymerization of ethene, propene and carbon monoxide was carried out with the catalyst precursors **3a–d**. In the test of each catalyst precursor the ethene pressure was systematically increased, while the propene concentration and carbon monoxide pressure were kept constant. The produced terpolymers were characterized by means of ^{1}H and ^{13}C NMR spectroscopy. The catalytic activity of the systems tested is discussed. The structure of the produced terpolymers is analyzed via NMR spectroscopy.

Keywords: C_s-symmetrical diphosphines; Terpolymerization; Ethene; Propene; Cationic palladium complexes

1. Introduction

Palladium(II) complexes of the kind [Pd(PˆP)S_2]X_2 (where PˆP is the chelating diphosphine ligand, S the solvent molecule and X is the weakly coordinating anion) when used as the catalyst made an interesting class of materials accessible comprising ethene and a simple 1-olefin together with carbon monoxide. The perfectly alternating structure of CO–ethene copolymers is altered by the introduction of the second olefinic monomer randomly distributed in the terpolymer chain. This structural aspect influences the solubility, the crystallinity and the melting point of these materials [1–3]. CO–ethene copolymers are white crystalline solids with high melting temperatures ($T_m \cong 260\,^\circ$C) that make them difficult to process. The introduction of small amounts of propene units decreases the melting point of the resulting materials [4], which are then more suitable for blow-molding or extrusion applications [5]. The first ethene–propene–carbon monoxide terpolymer was developed and commercialized by Shell under the trademark of Carilon® (Fig. 1) [1,6–9]. This material, obtained from a catalyst based on $Pd(OAc)_2$ and 1,3-bis(diphenylphosphino)propane [8–10], had a propene content of *ca.* 5–10%, estimated from the determination of the melting point.

Up to now it remains still unclear which factors are influencing the reactivity and the distribution of the two olefins in the terpolymer chain. Recent studies [11–13] showed that the propene content in the terpolymer chain was always lower than that introduced initially in the reaction mixture. Low propene content suggested a lower reactivity of this olefin compared to ethene toward the insertion. It was proposed [12,13] that propene insertion occurs randomly in the chain and the units are essentially isolated from each other at low concentration of inserted propene.

In this work, palladium complexes modified with the C_s-symmetric ligands **1a–d** (Fig. 2) of the kind [Pd(PˆP′)$(H_2O)_2$](OTf)$_2$ (PˆP′ = **1a–d**) were tested in the terpolymerization process. The relative reactivity of the two olefins in presence of each catalyst was evaluated. The stereochemical control achieved with the catalysts was qualitatively evaluated using ^{1}H and ^{13}C NMR spectroscopy.

* Corresponding author. Tel.: +41 44 63 23552; fax: +41 44 63 21162.
E-mail address: consiglio@chem.ethz.ch (G. Consiglio).

1381-1169/$ – see front matter © 2006 Elsevier B.V. All rights reserved.
doi:10.1016/j.molcata.2006.09.051

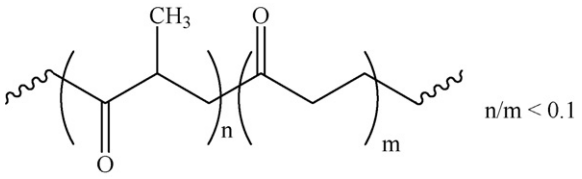

Fig. 1. Structure the commercialized terpolymer Carilon®.

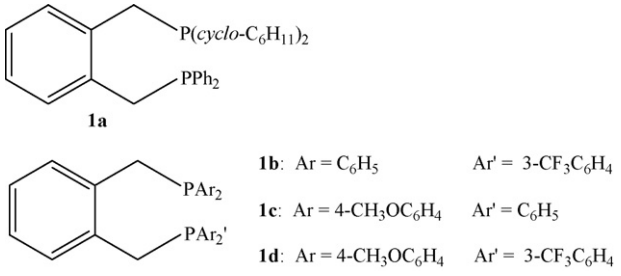

Fig. 2. Diphosphine ligands used.

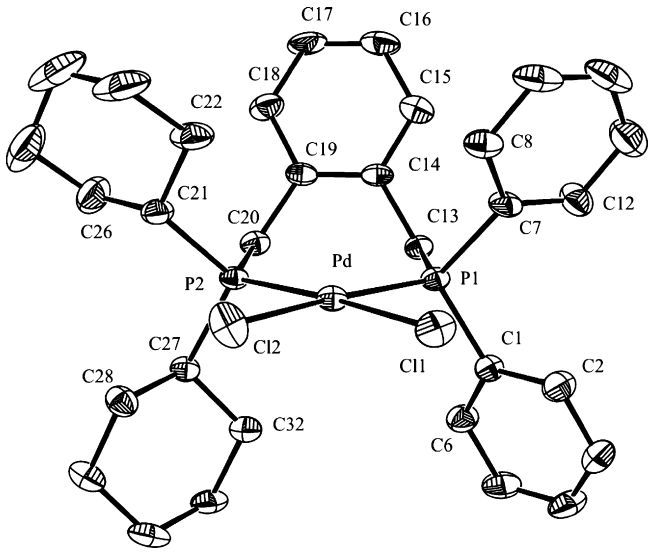

Fig. 3. ORTEP plot of **2a**. Thermal ellipsoids are set at the 30% probability level. Hydrogen atoms are omitted for clarity.

2. Results

2.1. Synthesis of the catalyst precursors

Several methods for the synthesis of palladium solvento complexes were reported [14,15]. The halide was abstracted from [$PdCl_2$(P^P′)] with the suitable silver salt according to the pathway described in Scheme 1.

The chelating ligand (**1a–d**, Fig. 2) replaces the nitrile in *trans*-[$(PhCN)_2PdCl_2$] heating the toluene solution of the precursor at 70 °C [16]. The isolated bis chloride complexes **2a–d** (**2a** = [$PdCl_2$(**1a**)]; **2b** = [$PdCl_2$(**1b**)]; **2c** = [$PdCl_2$(**1c**)]; **2d** = [$PdCl_2$(**1d**)]) were characterized by means of NMR spectroscopy, MALDI spectrometry and elemental analysis.

^{1}H NMR spectrum of the complex **2a** (**2a** = [$PdCl_2$(**1a**)]) showed at room temperature two broadened but distinct signals for each benzylic CH_2 group. The **CH_2**PCy_2 group gave two resonances at δ 2.40 and 2.72 (samples measured in $CDCl_3$), while **CH_2**PPh_2 was observed at 3.42 and 3.67 ppm. The $^{31}P\{^1H\}$ NMR exhibited two broadened peaks at δ 15.1 and 32.9 ppm for the two non-equivalent moieties at room temperature. This suggests that more than one conformation is populated at room temperature.

The diaquo palladium complexes **3a–d** (**3a–d** = [Pd(P^P′)$(H_2O)_2$]$(OTf)_2$; **3a** = [Pd(**1a**)$(H_2O)_2$]$(OTf)_2$; **3b** = [Pd(**1b**)$(H_2O)_2$]$(OTf)_2$; **3c** = [Pd(**1c**)$(H_2O)_2$]$(OTf)_2$; **3d** = [Pd(**1d**)$(H_2O)_2$]$(OTf)_2$) were obtained from the corresponding dichloride by scavenging the chloride anion with silver triflate. The synthesis was achieved with good yields (over 70%). The crystallization of these species was sometimes problematic, for the observed [16] tendency of the diaquo complexes to oil. Replacement of chloride with water produced a shift downfield of 10–15 ppm for the aryl substituted phosphorus atoms, and over 20 ppm for PCy_2. In the $^{31}P\{^1H\}$ NMR the phosphorus signals were broad. No coupling constant $^2J_{P-P}$ between the two non-equivalent moieties was observed for all the complexes **3a–d**.

2.2. Crystal structure of *2a* and *[Pd(1a)(CH3CN)(H2O)](OTf)2*

Single crystals suitable for X-ray analysis were obtained from the chloroform solution of the complexes **2a** and **4a** (**4a** = [Pd(**1a**)$(CH_3CN)(H_2O)$]$(OTf)_2$) with *n*-pentane at room temperature. ORTEP diagrams of the structures are displayed in Figs. 3 and 4, respectively.

A selection of bond lengths and angles is listed in Table 1. **2a** crystallizes in the monoclinic space group *P*2(1)/*c* as yellow platelets. A $CHCl_3$ molecule co-crystallizes with the complex. There are no intermolecular contacts significantly shorter than the sums of the *van der Waals* radii of the neighboring atoms. The geometry around the palladium is almost square planar. The distance of the chlorine atoms from the plane defined by P(1)–Pd(1)–P(2) is −0.0930 Å for Cl(1) and −0.0158 Å for Cl(2). Both the chlorine atoms are lying below the coordination plane. Bond lengths of the Pd–P bonds exhibit a significant

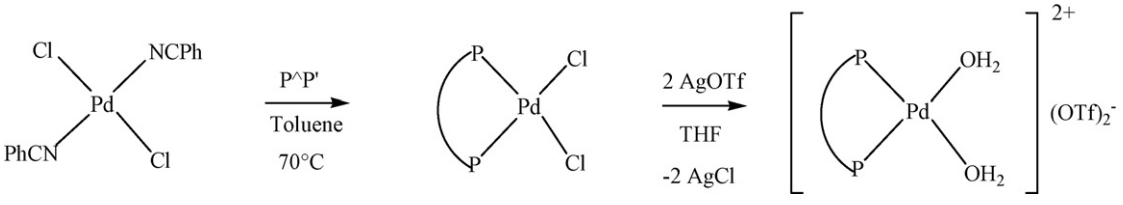

Scheme 1.

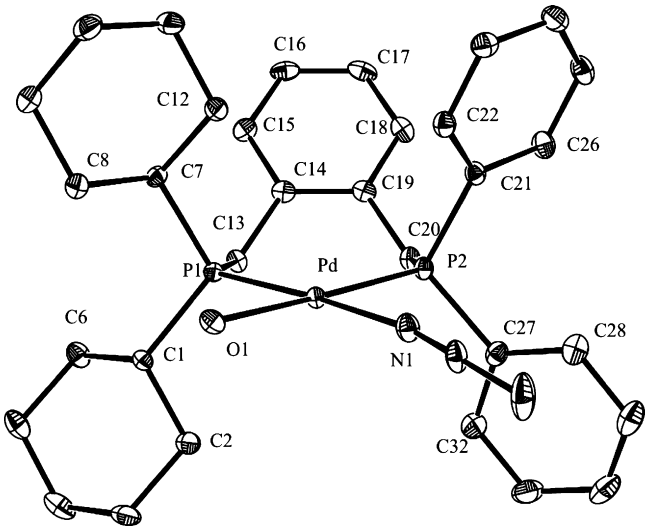

Fig. 4. ORTEP plot of **4a**. Thermal ellipsoids are set at the 30% probability level. Hydrogen atoms and counterions are omitted for clarity.

difference (Pd(1)–P(1) = 2.241(2) Å, Pd(1)–P(2) = 2.278(2) Å) but are within the range observed for other diphosphine palladium complexes such as [$PdCl_2$(dppe)] (dppe = 1,2-(diphenylphosphino)ethane)) [17], [$PdCl_2$ (dppb)] (dppb = 1,4-(diphenylphosphino)butane) [18], as well as palladium dichloride complexes modified with *Josiphos* C_1-symmetric derivatives [19]. The Pd–Cl distances display a very similar value (Pd(1)–Cl(1) = 2.339(2) Å, Pd(1)–Cl(2) = 2.333(2) Å) and, therefore, are not reflecting the different *trans* influence of the PCy_2 fragment. The bite angle P(1)–Pd(1)–P(2) is 99.94(8)° and it is larger than the ideal value of 90°. This shows the geometric constraint induced by the seven-membered chelate ring and it is similar to that of 103.08(3)° reported for the complex [Pd(C(O)Et)Cl(d^tbpx)] containing the same type of ligand (d^tbpx = 1,2-bis(di-*tert*-butylphosphinomethyl)benzene) [20]. Other more flexible 1,4 diphosphines formed complexes with smaller bite angle, as that of approximately 92.9° found for [Pd(SCN)(NCS)(dppb)] [21].

The benzylic atoms of the carbon backbone C(13) and C(20) are not perfectly coplanar with the plane defined by P(1)–Pd–P(2), but are lying 0.1679 Å and 0.2301 Å above it, respectively. The torsion angles P(2)–Pd(1)–P(1)–C(13) of 6.2(3)° and P(1)–Pd(1)–P(2)–C(20) of −8.6(3)° denote also the almost coplanar character of the two carbons. The seven-membered chelate ring is folded and adopts a skew boat conformation. The atoms C(13), C(14), C(15), C(16), C(17), C(18), C(19), C(20) define a least-squares plane, which forms an angle of 112.7° with the plane containing C(13), C(20), Pd(1), P(1), P(2). The orientation of the benzene ring, which lies above the coordination plane, can be further defined by the torsion angles P(1)–C(13)–C(14)–C(19) of −89.8(8)° and C(14)–C(19)–C(20)–P(2) of 78.5(9)°, respectively. The position of the substituents at the phosphorus atoms is described by the bond and torsion angles reported in Table 2. For each phosphorus atom one substituent lies above and the other below the coordination plane, respectively.

Originally synthesized as [Pd(**1a**)$(CH_3CN)_2$]$(OTf)_2$, the compound crystallized as [Pd(**1a**)$(CH_3CN)(H_2O)$]$(OTf)_2$, with the exchange of acetonitrile molecule with water. The displacement of acetonitrile with water had been already observed in

Table 1
Selected interatomic distances (Å) and angles (°) for **2a**

Bond length (Å)	
Pd(1)—P(1)	2.241(2)
Pd(1)—P(2)	2.278(2)
Pd(1)—Cl(2)	2.333(2)
Pd(1)—Cl(1)	2.339(2)
Bond angle (°)	
P(1)—Pd(1)—P(2)	99.94(8)
P(1)—Pd(1)—Cl(2)	172.23(8)
P(2)—Pd(1)—Cl(2)	87.82(8)
P(1)—Pd(1)—Cl(1)	83.97(8)
P(2)—Pd(1)—Cl(1)	175.48(8)
Cl(2)—Pd(1)—Cl(1)	82.26(9)

Table 2
Bond and torsion angles (°) describing the orientation of the substituents for **2a**

Bond angle (°)	
C(1)—P(1)—C(7)	107.3(4), Ph
C(21)—P(2)—C(27)	107.0(4), Cy
Torsion angle (°)	
Pd(1)—P(1)—C(7)—C(8)	−23.4(8), Ph
Pd(1)—P(1)—C(1)—C(2)	−95.7(7), Ph
Pd(1)—P(2)—C(21)—C(22)	48.6(7), Cy
Pd(1)—P(2)—C(27)—C(28)	78.4(6), Cy

Table 3
Selected interatomic distances (Å) and angles (°) for **4a**

Bond length (Å)	
Pd(1)—P(1)	2.2595(7)
Pd(1)—P(2)	2.2389(7)
Pd(1)—N(1)	2.082(3)
Pd(1)—O(1)	2.125(2)
Bond angle (°)	
N(1)—Pd(1)—O(1)	87.56(9)
N(1)—Pd(1)—P(2)	87.97(7)
O(1)—Pd(1)—P(2)	174.33(6)
N(1)—Pd(1)—P(1)	173.28(7)
O(1)—Pd(1)—P(1)	85.76(6)
P(2)—Pd(1)—P(1)	98.75(3)

Table 4
Structural parameters describing the position of the benzylic CH_2 groups and the orientation of the benzene ring with respect to the coordination plane for **4a**

Deviation of the benzylic C from the P(1)—Pd(1)—P(2) least-squares plane (Å)	
C(13)	−0.3487
C(20)	−0.3615
Orientation of the benzene ring with respect to the coordination plane	
Torsion angle (°)	
P(1)—C(13)—C(14)—C(19)	83.2(3)
C(14)—C(19)—C(20)—P(2)	−80.2(3)

A negative deviation implies that the C atom lies below the defined least-squares plane.

Table 5
Dihedral angle (°) between the planes defined by the numbered atoms for the complex **4a**

Plane 1	Plane 2	Dihedral angle (°)
C(13), C(14), C(15), C(16), C(17), C(18), C(19), C(20)	C(13), C(20), P(1), Pd(1), P(2)	123.8

Table 6
Bond and torsion angles (°) describing the orientation of the substituents for **4a**

Bond angle (°)	
C(1)–P(1)–C(7)	109.51(13), Cy
C(21)–P(2)–C(27)	108.92(14), Ph
Torsion angle (°)	
Pd(1)–P(1)–C(1)–C(2)	−49.1(2), Cy
Pd(1)–P(1)–C(7)–C(12)	37.5(2), Cy
Pd(1)–P(2)–C(21)–C(22)	−3.8(3), Ph
Pd(1)–P(2)–C(27)–C(32)	73.7(2), Ph

other cases [22] for the high affinity of water to the palladium center. Moreover, it was observed that the high binding constant of water to palladium can lead to displacements of ligands even when water is present at impurity level [23]. Co-crystallization of a chloroform molecule in the asymmetric unit also occurs. A selection of bonds and relevant angles is listed in Table 3.

[Pd(**1a**)$(CH_3CN)_2$]$(OTf)_2$ crystallizes in the monoclinic space group *P*2(1)/*n* as yellow platelets. The coordination sphere around the palladium is square planar with a slight distortion. The N(1) atom lies −0.0100 Å below the plane defined by P(1)–Pd(1)–P(2), while O(1) is found 0.1282 Å above it. The Pd–P bond lengths (Table 3) are comparable to those observed for the neutral dichloro complex of the same ligand and are within the expected range for *cis*-chelated diphosphines at a palladium(II) center [17,24–27].

The Pd–N(1) bond length in [Pd(**1a**)$(CH_3CN)(H_2O)$]$(OTf)_2$ is 2.082(3) Å, and is within the expected range found for complexes of the same kind such as [(dippf)Pd$(CH_3CN)H_2O$]$(OTf)_2$ (dippf = 1,1′-bis(diisopropylphosphino)ferrocene), [(*R*-BINAP)Pd$(CH_3CN)H_2O$]$(OTf)_2$ (BINAP = 1,1′-bis(diphenylphosphino)naphthalene) [22]. The bite angle of 98.75(3)° falls in the range expected for palladium complexes modified with *cis*-chelating diphosphine ligands and is slightly smaller than that of the neutral complex **2a**. The seven-membered ring adopts a skew boat conformation as in the corresponding palladium dichloride complex modified with the same ligand. The almost coplanar position of the benzylic carbons as well as the orientation of the benzene ring of the ligands show analogous structural features already observed in the neutral complex **2a**. Table 4 summarizes some relevant geometric features for the complex [Pd(**1a**)$(CH_3CN)(H_2O)$]$(OTf)_2$.

As in the case of the neutral complex **2a**, the folding of the chelate ring can be described by the angle formed between the least-squares plane containing the benzene ring and the least-squares plane defined by the benzylic carbons, the phosphorus atoms and the metal. Table 5 defines the corresponding planes and the angle formed by their intersection. The position of the

Table 7
Terpolymerization of ethene, propene and carbon monoxide catalyzed by **3a**–**d**

Catalyst	Ethene (mol)[a]	Ethene/propene ratio	Reaction time (h)	Productivity (g terpol/(g_{Pd} h))	x_p[b]	M_n[c] ($\times 10^{-3}$)
3a	0.0183	0.039	2	149	0.600	2.3
3a	0.0994	0.214	2	395	0.100	3.0
3a	0.1273	0.274	2	448	0.061	n.d.
3a	0.2096	0.450	1.5	510	0.048	4.1
3a	0.2515	0.541	1.5	580	0.025	2.3
3b	0.0359	0.077	2	775	0.622	2.2
3b	0.0712	0.153	2	832	0.159	4.1
3b	0.1608	0.346	2	810	0.129	7.6
3b	0.2108	0.453	1.6	855	0.052	13.5
3b	0.2538	0.546	1	840	0.012	14.9
3c	0.0305	0.066	2	435	0.384	3.9
3c	0.0935	0.201	2	758	0.099	10.2
3c	0.1184	0.255	2	980	0.093	4.4
3c	0.2138	0.460	1.5	1080	0.073	5.0
3c	0.2682	0.577	1.5	1173	0.036	3.6
3d	0.0301	0.065	2	324	0.566	1.6
3d	0.0684	0.147	2	337	0.317	8.4
3d	0.1153	0.248	2	371	0.118	16.0
3d	0.2203	0.474	2	306	0.074	10.0
3d	0.2619	0.563	2	383	0.053	12.0

Reaction conditions: 0.03 mmol catalyst precursor (**3a**–**d**); 19 g (0.45 mol) propene; 80 bar carbon monoxide; 273 mg 1,4-naphtoquinone (1.73 mmol); THF: 75 ml; MeOH: 4.5 ml. The reactions were carried out in a 250 ml stainless steal autoclave at $T = 44\,^{\circ}C$. n.d., not determined.

[a] Moles of ethene in the reaction mixture.

[b] Propene content (expressed as molar fraction) in the terpolymers, calculated by integration of ^1H NMR spectra.

[c] Averaged molecular weight.

substituents at the phosphorus atoms is described through the bond and torsion angles reported in Table 6. Similarly to **2a**, for each phosphorus atom one substituent lies above and the other below the coordination plane, respectively.

2.3. Terpolymerization experiments

Terpolymerization experiments were carried out by dissolving 0.03 mmol of the catalyst precursors **3a–d** [Pd(P^P′)$(H_2O)_2$]$(OTf)_2$ (where P^P′ = **1–4a**; **3a** (**1a**), **3b** (**1b**), **3c** (**1c**), **3d** (**1d**), Fig. 2) in 75 ml of dry THF and 4.5 ml of dry MeOH in the presence of 273 mg (1.73 mmol) of 1,4-naphtoquinone. The amount of propene was kept constant during all the experiments (19 g, 0.45 mol), as well as carbon monoxide pressure (80 bar). The amount of ethene was progressively increased in the feed up to *ca.* 0.26 mol, so that the maximum ratio ethene/propene was close to 0.6.

The catalyst precursors tested in the terpolymerization reaction were previously studied in the copolymerization of carbon monoxide and propene [28]. All the systems afforded stereo- and regioregular copolymers, displaying differences only in the catalytic activity. The ligands **1–4a** investigated in this work present the same steric requirements but have different electronic properties at the donor atoms. The catalytic performance of the systems **3a–d**, the propene content and the averaged molecular weight of the produced terpolymers are reported in Table 7.

2.4. Catalytic activity

The catalytic activity in the terpolymerization process of all the investigated systems **3a–d** was higher than that observed in the propene–CO copolymerization carried out with the same catalyst precursors [28]. This indicates a different reactivity of the two olefinic monomers. In order to produce only modest changes in the catalytic mixture, the terpolymerization process had a maximum duration of 2 h, while keeping the conversion low (less than 5%). The productivity was calculated as the amount of material produced (g) per gram of palladium per hour (g terpol/(g_{Pd} h)). Fig. 5 shows the productivity values plotted as a function of the ethene moles present initially in the feed.

The activity of the catalyst precursors **3b** and **3d** modified with the ligands **1b** and **1d** remained essentially constant with increasing the ethene concentration in the reaction mixture. Productivity values for **1b** were two times larger than for **1d**, reflecting the different efficiency already encountered in the copolymerization reaction. In the CO–propene copolymerization **3d** was the less active system among the series **3a–d**. The catalyst precursors modified with **1a** and **1c** exhibited an increase of the productivity with the ethene content in the feed. **3c** became the most efficient of the series when the ethene content in the reaction mixture was *ca.* 0.12 mol (ethene:propene molar ratio ≥0.25). **1b** and **1c** displayed comparable productivity in the CO–propene copolymerization, when the reaction was carried out in THF (126 and 123 g copolymer/(g_{Pd} h), respectively) [28]. **1a** increased the productivity by almost a factor of 4 when the ratio ethene:propene in the feed was increased from 0.04 (productivity = 149 g terpolymer/(g_{Pd} h)) to 0.56 (productivity = 580 g terpolymer/(g_{Pd} h)). For the catalyst precursor modified by **1c** the catalytic activity improved only by a factor 2.7 when increasing the ethene:propene ratio from 0.07 (productivity = 435 g terpolymer/(g_{Pd} h)) to 0.6 (productivity = 1173 g terpolymer/(g_{Pd} h)). The higher basicity of **1a** seemed to favor the affinity to ethene with the increase of its concentration in the feed, even though the donor atoms were functionalized with sterically hindered *cyclo*-hexyl groups at one moiety.

2.5. NMR analysis of the terpolymers

Ethene–propene–CO terpolymers were analyzed by means of NMR spectroscopy. A typical ^{1}H NMR is shown in Fig. 6.

The relative concentration of ethene and propene units in the terpolymers was determined from the integration of the signals in the ^{1}H NMR according to the procedure described previously [29]. It was proposed [13] that the region of methyl group is particularly sensitive to the distribution of the propene units in the terpolymer chain. When the resolution of the spectrum is satisfactory, two distinct doublets can be observed. The doublet upfield was assigned to isolated propene units [12] and was therefore prevailing in samples with low concentration of propene in the chain. At higher concentration of propene, a doublet appeared at lower fields, which was assigned to the propene *n*-ads of an order higher than 1. This signal overlapped the corresponding methyl peak of a poly[1-methyl-2-oxo-propanediyl]

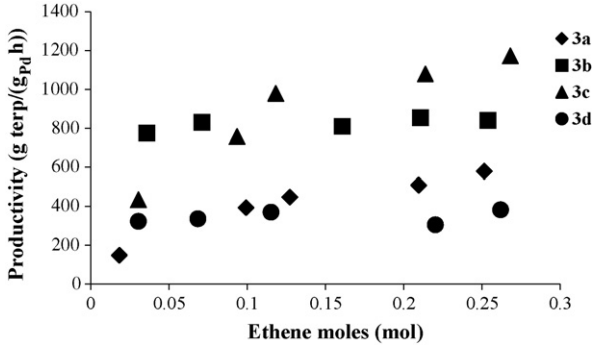

Fig. 5. Productivity (g terpolymer/(g_{Pd} h)) of the catalyst precursors **3a–d** as a function of the ethene moles present in the feed.

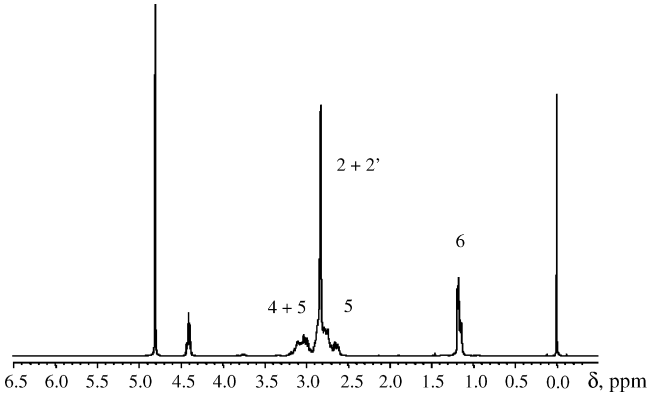

Fig. 6. ^{1}H NMR spectrum (500 MHz, δ ppm, HFIP-d_2) for an ethane–propene–CO terpolymer sample with a propene content of 31.7%.

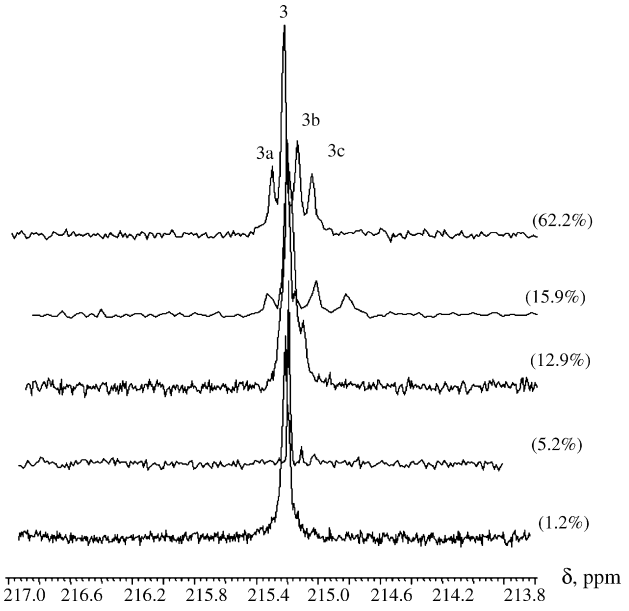

Fig. 7. ^{13}C NMR (125 MHz, δ ppm, HFIP-d_2) region of the carbonyl groups of type 3 of the [$CH_2CH_2C(O)$] units in the terpolymers obtained with the catalyst precursor **3b**. Chemical shifts are referred to TMS in HFIP-d_2. Propene content is indicated in brackets.

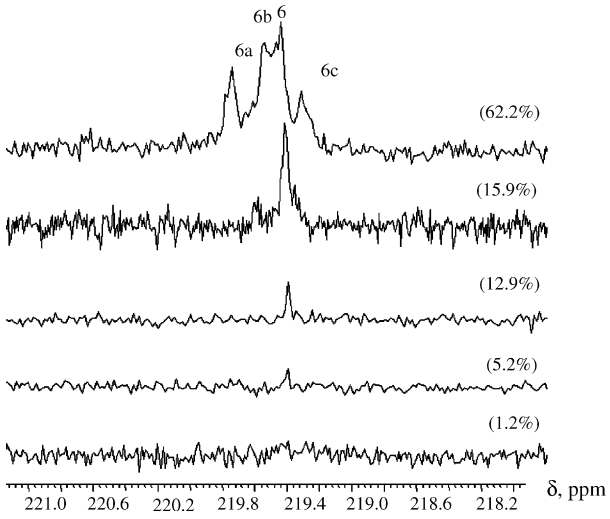

Fig. 8. ^{13}C NMR (125 MHz, δ ppm, HFIP-d_2) region of the carbonyl groups of type 6 of the [$(CH_3)CHCH_2C(O)$] units (primary insertion of propene indicated arbitrarily) as in the terpolymers obtained with the catalyst precursor **3b**. Chemical shifts are referred to TMS in HFIP-d_2. Propene content is indicated in brackets.

[12]. Integration of these two types of methyl groups afforded an estimation of the propene distribution in the terpolymer chain. The stacked plot of the ^{1}H NMR spectra for two samples of terpolymer obtained with **3a** with propene content of 60 and 6.1%, respectively, appears in Fig. 1 of the Supplementary material.

A typical ^{13}C NMR spectrum of a terpolymer sample is displayed in Fig. 2 of the Supplementary material.

According to the assignment reported previously [1], resonances labeled with 6 (Fig. 3; Supplementary material) are due to carbonyl group of the repeating unit [(O)C–CH–(CH_3)–CH_2]. Insertion of ethene generates the [CH_2–CH_2–C(O)] unit. The resonances at *ca.* 215 ppm (labeled with 3 in Fig. 7) are attributed to the carbonyl groups. The stacked plot of the carbonyl region of the [CH_2–CH_2–C(O)–CH_2–CH_2] unit for the terpolymers produced with **3b** is displayed in Fig. 7. The sample with the lower propene content (1.2%) showed a major peak at *ca.* 215.2 ppm. The region presented a differentiation of the main peak into a four-signal pattern in materials with increasing the propene concentration (above *ca.* 13%). In the sample containing 15.9% of propene the differentiation is already clearly visible (Fig. 7).

A magnification of the carbonyl region of the ^{13}C NMR spectrum containing the propene–CO units is shown in Fig. 8.

The modest solubility of some of the samples in HFIP-d_2 did not allow the use of concentrated samples for the acquisition of the NMR spectra. Therefore, the signal to noise ratio was sometimes not optimal. The signal describing the carbonyl groups of units resulting from propene insertion is not visible in the spectra of materials containing 1.2% of the olefin, and hardly observable with 5.2% of propene content.

In the sample containing 15.9% of propene a three-signal pattern can be observed. In the sample with higher propene content (62.2%) the main peak, labeled as 6 in Fig. 8, is flanked by another signal, labeled as 6b, of comparable intensity. The peak 6b (Fig. 8), which has a negligible intensity in the sample containing 15.9% of propene, is comparable to signal 6 in the material with higher propene content. The region contains two other peaks of smaller intensity (Fig. 8), indicated as 6a and 6c, respectively.

2.6. Distribution of the olefins in the terpolymers

The relative concentration of ethene and propene in a terpolymer sample can be calculated from the integration of the ^{1}H NMR spectrum [13]. Fig. 9 shows the concentration of propene in the terpolymer samples obtained with the catalyst precursors **3a**–**d** as a function of the ethene content in the reaction mixture.

The increase of the ethene concentration in the feed corresponds to a decrease of the propene content in the terpolymers. At lower concentration of ethene, the catalytic system modified with the ligand **1c** seemed to be more sensitive to the presence of the olefin. When the feed contained less than 0.05 mol of ethene, **3c** produced terpolymers with 38.4% of propene content, while the percentage was 60, 62.2 and 56.6% for **3a**, **3b** and **3d**, respec-

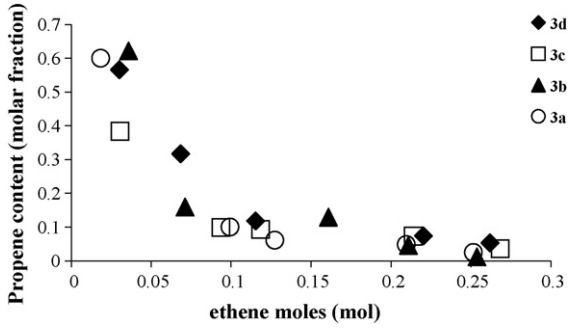

Fig. 9. Propene content in the terpolymer chain vs. ethene concentration in the reaction mixture, expressed as moles of the olefin. The trend for all the samples obtained with the catalyst precursors **3a**–**d** is reported.

tively. The catalytic system containing **1c** inserted propene to a lower extent than the other systems tested, even when the amount of propene was 15.2 times that of ethene.

At higher concentration of ethene in the reaction mixture all the catalytic systems displayed a similar trend. The ratio propene:ethene in the feed was decreased from *ca.* 25 to 1.7. When the concentration of ethene in the reaction feed reached half of that of propene, the corresponding terpolymers showed a propene content equal or less than 7.4%.

3. Discussion

3.1. Catalytic activity

The productivity values of the terpolymerization for the systems **3a–d** were higher than those found for the copolymerization reaction [28]. All the systems did not present significant variations of the productivity with increasing ethene concentration in the reaction mixture. The efficient regiochemical control displayed by the systems **3a–d** in the copolymerization was achieved probably through a sequence of primary insertions of the propene units [30,31]. The intermediates formed after the olefin insertion (ethene and/or propene) in the terpolymerization process presented comparable steric hindrance and should display a similar reactivity in the migratory insertion of carbon monoxide. Therefore, the difference in reactivity of the two olefinic monomers should reflect the relative rates of complexation and/or insertion. The catalyst precursor **3d** was the less active in the series. It displayed low efficiency in the copolymerization of propene and carbon monoxide, with a productivity of 15 g copolymer/(g_{Pd} h). The productivity trend for the systems **3a–d** in the terpolymerization process was consistent with the activity order observed in the copolymerization. The reasons for the modest activity of the system **3d** are not completely understood. Electronic factors should control the migratory insertion of the olefin into a Pd–acyl bond or that of CO into a Pd–alkyl bond. According to the proposed mechanism [29], this might slow down the reaction, as the vacancy for the coordination of CO is not readily available.

The presence of more stereoisomers after carbonylation and propene insertion was shown for the C_s-symmetrical diphosphine ligands **1b–d** (Fig. 2) investigated by means of NMR spectroscopy [32,33]. It is likely that the same stereoisomers exist in the steps of the polymerization. In reactions requiring a series of migrations, as in a polymerization reaction where the growing chain moves from one site to the other, the faster catalysts should be those containing symmetric diphosphines or bypiridines [34]. Considering the catalysts **3a–d**, **3c** and **3a**, which contain the ligands **1c** and **1a**, respectively, were the most active systems. The corresponding ligands presented the smaller electronic differentiation between the dentates, when compared to **1b** and **1d**.

3.2. Distribution of the monomers in the terpolymer chain

According to NMR, in samples with low propene content the [$(CH_3)CHCH_2C(O)$] chain elements tend to be isolated. With the increase of propene concentration, more propene units are close to each other (Fig. 1; Supplementary material). For this kind of samples the concentration of the type-6 carbonyl group decreases, while the carbonyl groups of the kind 1, 2 and 4 occurs with increasing frequency. When the ^{13}C NMR spectrum of a terpolymer sample with 62.2% of propene is considered (Fig. 8), the signal labeled with 6, which is already visible in samples with *ca.* 5% propene content, is attributed to isolated propene units. The peak 6b is only detected in the sample with high propene content. This kind of signal can be assigned to longer chain elements of the type [$(CH_3)CHCH_2C(O)$] resulting from subsequent propene insertions.

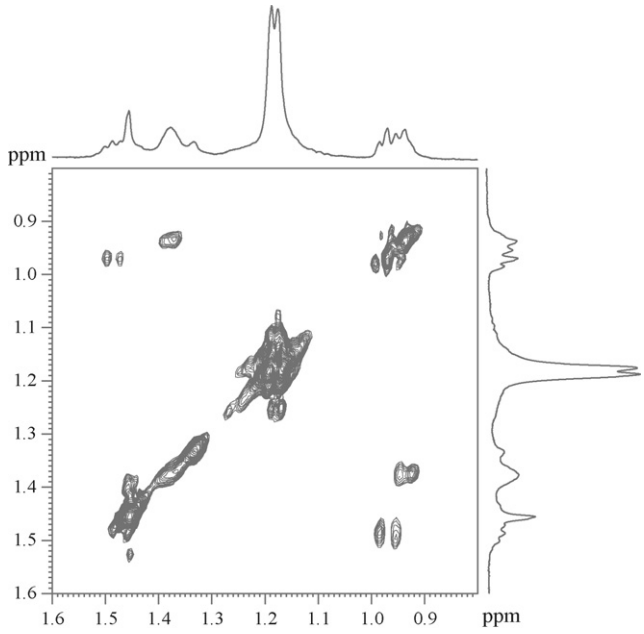

Fig. 10. Detail of a ^{1}H-COSY (δ ppm, HFIP-d_2, 298 K) spectrum in the alkyl groups region for a terpolymer sample obtained with the catalyst precursor **3c** and containing 3.6% of propene.

As far as the [$CH_2CH_2C(O)$] units are concerned, the signal labeled with 3 in the ^{13}C NMR spectrum (Fig. 7) is assigned to carbonyl carbons of type 3, which are the most abundant in materials with low propene concentration. The resonances labeled in the ^{13}C NMR spectrum as 3a, 3b and 3c (Fig. 7) describe [$CH_2CH_2C(O)$] units surrounded in various ways by [$(CH_3)CHCH_2C(O)$] chain elements. Their occurrence increases with the propene content in the reaction mixture. Propene insertion occurs essentially random in the chain [13].

In some cases the ^{1}H-COSY spectrum presents two types (surrounded by different environments) of CH_3 groups directly bound to CH_2 units (cross peaks in Fig. 10). The occurrence of these CH_2 groups at δ *ca.* 1.40–1.50 ppm shows that they are not bound to carbonyl groups, which would shift downfield the resonances of 1.40–1.30 ppm (Fig. 6: the chemical shift, referred to HFIP-d_2, of the CH_2 protons labeled as 2 and 2′ is at δ 2.80 ppm). This suggests the presence of two vicinal ethene units, as the result of a double insertion. The [$CH_2CH_2CH_2CH_3$] unit can be located at the beginning or at the end of the terpolymer chain.

4. Conclusions

Neutral dichloro **2a–d** and cationic bis-solvento **3a–d** palladium complexes containing non-symmetric diphosphine ligands were synthesized and characterized. The test of the cationic catalyst precursors in the terpolymerization of propene, ethene and carbon monoxide showed the productivity trend already observed in the copolymerization process. In particular, higher basicity of the phosphorus moieties improves the catalytic performance of the systems in the terpolymerization.

5. Experimental

5.1. General information

All reactions with air- or moisture-sensitive compounds were carried out under nitrogen or argon using standard Schlenk techniques or a glove box. The synthesis of the ligands **1a–d** had been previously described [28].

Silver trifluoromethansulfonate was purchased from Fluka.

Benzonitrile was of "puriss." grade and was purchased from Fluka. Toluene, tetrahydrofuran, dichloromethane, and acetonitrile used for the synthesis were of "puriss." grade, dried over molecular sieves ("crown cap") and were purchased from Fluka. All the solvents used for recrystallization were of "puriss." quality, purchased from Fluka and purified according to standard procedures. *Trans*-[$PdCl_2(NCPh)_2$] was prepared according to published procedures [35]. $CDCl_3$ and HFIP-d_2 (1,1,1,3,3,3-Hexafluoro-2-propanol-d_2) were purchased from Dr. Glaser AG and Cambridge Isotope Laboratories, respectively. Propene (purity grade 2.8) and ethene (purity grade 3.5) were purchased from Linde. Carbon monoxide (purity grade 4.7) was purchased from Pan Gas.

The ^{1}H-, ^{13}C-, ^{31}P{^{1}H}, ^{19}F{^{1}H}- and 2D spectra were measured in $CDCl_3$ or C_6D_6 and recorded on a Bruker Avance 200 (frequency in MHz: ^{1}H: 200.13; ^{31}P: 81.01; ^{19}F: 188.31) or Bruker Avance 500 (frequency in MHz: ^{1}H: 500.13; ^{13}C: 125.77; ^{31}P: 202.45). Chemical shifts are given in parts per million (ppm) relative to TMS (internal standard) or the solvent residual peak for ^{1}H and ^{13}C NMR, and relative to 85% H_3PO_4 (external standard) for ^{31}P{^{1}H} NMR. ^{19}F NMR spectra are calibrated to CCl_3F as the internal standard. The coupling constants J are given in hertz. The multiplicity is denoted by the following abbreviations: s: singlet; d: doublet; t: triplet; q: quartet; qt: quintet; sx: sextet; sp: septet; m: multiplet; dd: doublet of doublets; dq: doublet of quartets; br: broad.

Elemental analysis (EA) was performed by the service of "Laboratorium für Organische Chemie" of the ETH Zurich. The mass spectra (MS) were recorded by the service of the "Laboratorium für Organische Chemie" of the ETH Zurich on a Finnigan TSQ 7000 mass spectrometer (electrospray ionization, ESI) and on an IonSpec Ultima 4.7 Fourier Transform mass spectrometer (MALDI). The molecular ion is shown as [M^+]. The mass values are expressed using the ratio mass/charge (m/z) as the unit. The intensities, in percentage, relative to the basis peak are displayed in brackets.

5.2. Synthesis of the dichloro palladium complexes [$PdCl_2$(P^P′)] 2a–d

5.2.1. General procedure [16]

A solution of [$PdCl_2(NCPh)_2$] (1 equiv.) in toluene (60–90 ml) was heated to 70 °C. To this red–brown solution a solution of the diphosphine ligand (1.02–1.03 equiv.) in toluene (20–30 ml) was added dropwise. The solution became brighter and a yellow precipitate formed. The suspension was held for another 2.5 h at this temperature and was then cooled to room temperature. Addition of *n*-pentane completed the precipitation. The complex was recovered from filtration, washed with diethyl ether and dried overnight in HV.

5.2.2. **2a** ([$PdCl_2$(1a)])

Quantitative yield of a yellow powder.

- ^{1}H NMR: (500 MHz, $CDCl_3$, 25 °C): δ 1.26–1.78 (br, 44 H, Cy-H), 2.40 (br, 2H, CH_2, CH_2PCy_2), 2.72 (d, 2H, CH_2; $^2J_{H-P}$ = 10.30 Hz, CH_2PCy_2), 3.42 (br, 2H, CH_2PPh_2), 3.67 (br, 2H, CH_2PPh_2), 6.04 (m, 1H, C_6H_4), 6.86 (m, 1H, C_6H_4), 7.15 (m, 1H, C_6H_4), 7.28 (m, 2H, C_6H_4 and Ph), 7.42–7.50 (m, 6H, Ph), 7.85 (br, 3H, Ph).
- ^{31}P{^{1}H} NMR: (202 MHz, $CDCl_3$, 25 °C): δ 15.1 (d, PPh_2; $^2J_{P-P}$ = 8.30 Hz), 32.9 (d, PCy_2; $^2J_{P-P}$ = 8.30 Hz).
- Anal. Calcd. for $C_{32}H_{40}P_2Cl_2Pd$ (663.94): C, 57.89; H, 6.07. Found: C, 57.95; H, 6.20.
- MS (MALDI): 589 ([M − 2Cl4H]$^+$, 100), 506 ([M − 2Cl Cy]$^+$, 50), 289 (78).

5.2.3. **2b** ([$PdCl_2$(1b)])

Yield: 76 %, brown–yellow powder.

- ^{1}H NMR: (500 MHz, CD_2Cl_2, 25 °C): δ 3.88 (s, 2H, CH_2PPh_2), 3.91 (s, 2H, $CH_2P(3\text{-}CF_3C_6H_4)_2$), 6.10 (m, 1H, C_6H_4), 6.22 (m, 1H, C_6H_4), 6.90 (m, 2H, C_6H_4), 7.51–7.58 (m, 4H, Ph), 7.60–7.65 (m, 2H, 3-$CF_3C_6H_4$), 7.68–7.74 (m, 2H, 3-$CF_3C_6H_4$), 7.87–7.95 (m, 6H, Ph), 8.05 (m, 2H, 3-$CF_3C_6H_4$), 8.12–8.19 (m, 2H, 3-$CF_3C_6H_4$).
- ^{31}P{^{1}H} NMR: (202 MHz, CD_2Cl_2, 25 °C): δ 16.7 (d, $P(3\text{-}CF_3C_6H_4)_2$; $^2J_{P-P}$ = 6.67 Hz), 17.4 (d, PPh_2, $^2J_{P-P}$ = 6.67 Hz).
- ^{19}F NMR: (188 MHz, CD_2Cl_2, 25 °C): δ −61.1 (s, CF_3).
- Anal. Calcd. for $C_{34}H_{26}F_6P_2Cl_2Pd$ (787.84): C, 51.83; H, 3.33. Found: C, 52.39; H, 3.48.
- MS (MALDI): 753 ([M − Cl]$^+$, 80), 715 ([M − 2Cl2H]$^+$, 100).

5.2.4. **2c** ([$PdCl_2$(1c)])

Yield: 88%, yellow powder.

- ^{1}H NMR: (500 MHz, CD_2Cl_2, 25 °C): δ 3.77 (d, 2H, $CH_2P(4\text{-}OCH_3C_6H_4)_2$; $^2J_{H-P}$ = 10.80 Hz), 3.81 (d, 2H, CH_2PPh_2; $^2J_{H-P}$ = 10.80 Hz), 3.87 (s, 6H, OCH_3), 6.13 (m, 1H, C_6H_4), 6.20 (m, 1H, C_6H_4), 6.82–6.92 (m, 2H, C_6H_4), 6.96–7.03 (m,

4H, 4-$OCH_3C_6H_4$), 7.45–7.56 (m, 6H, Ph), 7.77–7.85 (m, 4H, 4-$OCH_3C_6H_4$), 7.86–7.94 (m, 4H, Ph).

- $^{31}P\{^1H\}$ NMR: (202 MHz, CD_2Cl_2, 25 °C): δ 15.5 (d, P(4-$OCH_3C_6H_4$)$_2$; $^2J_{P-P}$ = 6.54 Hz), 17.4 (d, PPh_2; $^2J_{P-P}$ = 6.54 Hz).
- Anal. Calcd. for $C_{34}H_{32}O_2P_2Cl_2Pd$ (711.89): C, 57.36; H, 4.53; C, 57.92; H, 4.59.
- MS (MALDI): 549 ($[M - 2ClPhCH_3]^+$, 100).

*5.2.5. **2d** ([$PdCl_2$(1d)])*

Yield: 81%, brown–yellow powder.

- ^1H NMR: (500 MHz, $CDCl_3$, 25 °C): δ 3.81 (s, 2H, CH_2P(3-$CF_3C_6H_4$)$_2$), 3.83 (s, 2H, CH_2P(4-$OCH_3C_6H_4$)$_2$), 3.89 (s, 6H, OCH_3), 6.07 (m, 1H, C_6H_4), 6.27 (m, 1H, C_6H_4), 6.85–7.03 (m, 6H, C_6H_4 and 4-$OCH_3C_6H_4$), 7.59–7.66 (m, 2H, 3-$CF_3C_6H_4$), 7.76–7.86 (m, 4H, 4-$OCH_3C_6H_4$), 7.95–8.02 (m, 2H, 3-$CF_3C_6H_4$), 8.11–8.20 (m, 2H, 3-$CF_3C_6H_4$).
- $^{31}P\{^1H\}$ NMR: (202 MHz, $CDCl_3$, 25 °C): δ 15.7 (d, P(4-$OCH_3C_6H_4$)$_2$; $^2J_{P-P}$ = 5.59 Hz), 17.1 (d, P(3-$CF_3C_6H_4$)$_2$; $^2J_{P-P}$ = 5.59 Hz).
- ^{19}F NMR: (188 MHz, $CDCl_3$, 25 °C): δ −61.1 (s, CF_3).
- Anal. Calcd. for $C_{36}H_{30}O_2F_6P_2Cl_2Pd$ (847.89): C, 51.00; H, 3.57. Found: C, 51.79; H, 3.90.

*5.3. Synthesis of the diaquo bis-triflate palladium complexes [Pd(P^P′)(H_2O)$_2$](OTf)$_2$ **3a–d***

5.3.1. General procedure [16]

A solution of AgOTf (*ca.* 2.2–2.5 equiv.) in THF (60–80 ml) was added dropwise under exclusion of light to a solution of **2a–d** in THF (30–40 ml). The reaction mixture was stirred for *ca.* 2 h at room temperature, and then it was filtered over Celite to remove the precipitated AgCl. The filtrate was concentrated in vacuum and added to cold (0 °C) *n*-pentane to precipitate the complex. The precipitate was recovered by filtration, washed with *n*-pentane and dried overnight under HV.

In some cases only an oily product was obtained after precipitation with *n*-pentane or attempts of recrystallization of the complexes.

*5.3.2. **3a** ([Pd(**1a**)(H_2O)$_2$](OTf)$_2$)*

Yield: 75%, yellow.

^1H NMR: (500 MHz, $CDCl_3$, 25 °C): δ 1.12–1.36 (m, 11H, Cy), 1.52–1.84 (m, 11H, Cy), 2.11 (br, 2H, CH_2PCy_2), 2.31 (br, 2H, CH_2PCy_2), 3.36 (br, 2H, CH_2PPh_2), 3.42 (br, 2H, CH_2PPh_2), 5.99 (m, 1H, C_6H_4), 6.83 (m, 1H, C_6H_4), 7.12 (m, 1H, C_6H_4), 7.24 (m, 1H, C_6H_4), 7.40–7.48 (m, 4H, Ph), 7.51–7.58 (m, 2H, Ph), 7.59–7.75 (m, 4H, Ph).
$^{31}P\{^1H\}$ NMR: (202 MHz, $CDCl_3$, 25 °C): δ 27.3 (d, PPh_2; $^2J_{P-P}$ = 6.50 Hz), 54.1 (br, PCy_2).
^{19}F NMR (188 MHz, $CDCl_3$, 25 °C): δ −78.7 (s, free triflate).
Anal. Calcd. for $C_{34}H_{44}O_8F_6P_2S_2Pd$ (927.18): C, 44.04; H, 4.78. Found: C, 44.68; H, 4.91.

*5.3.3. **3b** ([Pd(**1b**)(H_2O)$_2$](OTf)$_2$)*

Yield: 78%, yellow.

- ^1H NMR: (500 MHz, $CDCl_3$, 25 °C): δ 3.98 (s, 2H, CH_2PPh_2), 4.12 (s, 2H, CH_2P(3-$CF_3C_6H_4$)$_2$), 4.13–4.52 (br, 4H, H_2O), 6.15 (m, 1H, C_6H_4), 6.33 (m, 1H, C_6H_4), 6.88–7.02 (m, 2H, C_6H_4), 7.47–7.69 (m, 8H, Ph and 3-$CF_3C_6H_4$), 7.74–8.00 (m, 8H, Ph and 3-$CF_3C_6H_4$), 8.17–8.34 (m, 2H, 3-$CF_3C_6H_4$).
- $^{31}P\{^1H\}$ NMR: (202 MHz, $CDCl_3$, 25 °C): δ 27.6 (br, P(3-$CF_3C_6H_4$)$_2$, 29.9 (br, PPh_2).
- ^{19}F NMR: (188 MHz, $CDCl_3$, 25 °C): δ −61.1 (s, CF_3), −78.7 (s, free triflate).
- Anal. Calcd. for $C_{36}H_{30}O_8F_{12}P_2S_2Pd$ (1051.08): C, 41.14; H, 2.88. Found: C, 41.95; H, 2.96.
- MS (ESI): 753 ($[M]^+$, 92), 629 (100).

*5.3.4. **3c** ([Pd(**1c**)(H_2O)$_2$](OTf)$_2$)*

Yield: 84%, yellow.

- ^1H NMR: (500 MHz, $CDCl_3$, 25 °C): δ 3.80 (s, 6H, OCH_3), 3.94 (d, 2H, CH_2P(4-$OCH_3C_6H_4$)$_2$; $^2J_{H-P}$ = 11.31 Hz), 3.98 (d, 2H, CH_2PPh_2; $^2J_{H-P}$ = 11.31 Hz), 6.29 (m, 1H, C_6H_4), 6.34 (m, 1H, C_6H_4), 6.90–7.00 (m, 6H, C_6H_4 and 4-$OCH_3C_6H_4$), 7.47–7.56 (m, 4H, Ph), 7.57–7.64 (m, 2H, Ph), 7.64–7.73 (m, 4H, 4-$OCH_3C_6H_4$), 7.73–7.82 (m, 4H, Ph).
- $^{31}P\{^1H\}$ NMR: (202 MHz, $CDCl_3$, 25 °C): δ 29.1 (br, PPh_2), 30.2 (br, P(4-$OCH_3C_6H_4$)$_2$).
- ^{19}F NMR: (188 MHz, $CDCl_3$, 25 °C): δ −78.7 (s, free triflate).
- Anal. Calcd. for $C_{36}H_{36}O_{10}F_6P_2S_2Pd$ (975.17): C, 44.34; H, 3.72. Found: C, 44.68; H, 3.91.

*5.3.5. **3d** ([Pd(**1d**)(H_2O)$_2$](OTf)$_2$)*

Yield: 89%, yellow.

- ^1H NMR: (500 MHz, $CDCl_3$, 25 °C): δ 3.86 (s, 6H, OCH_3), 4.14–4.32 (br, 4H, CH_2P(4-$OCH_3C_6H_4$)$_2$ and CH_2P(3-$CF_3C_6H_4$)$_2$), 6.17 (m, 1H, C_6H_4), 6.41 (m, 1H, C_6H_4), 6.93 (m, 1H, C_6H_4), 6.98–7.08 (m, 5H, C_6H_4 and 4-$OCH_3C_6H_4$), 7.69–7.84 (m, 8H, 4-$OCH_3C_6H_4$ and 3-$CF_3C_6H_4$), 7.84–7.90 (m, 2H, 3-$CF_3C_6H_4$), 8.14–8.25 (m, 2H, 3-$CF_3C_6H_4$).
- $^{31}P\{^1H\}$ NMR: (202 MHz, $CDCl_3$, 25 °C): δ 29.1 (br, P(3-$CF_3C_6H_4$)$_2$), 30.6 (br, P(4-$OCH_3C_6H_4$)$_2$).
- ^{19}F NMR: (188 MHz, $CDCl_3$, 25 °C): δ −61.1 (s, CF_3), −78.7 (s, free triflate).
- Anal. Calcd. for $C_{38}H_{34}O_{10}F_{12}P_2S_2Pd$ (1111.16): C, 41.07; H, 3.08. Found: C, 41.48; H, 3.21.

*5.4. Synthesis of the diacetonitrile bis-triflate palladium complex [Pd(**1a**)(CH_3CN)$_2$](OTf)$_2$ **4a***

The complex was prepared according to the procedure reported in the literature [22].

A solution of AgOTf (116 mg, 0.452 mmol, 2.5 equiv.) in 10 ml of CH_2Cl_2 and 2 ml of CH_3CN was added to a solution of **2a** (120 mg, 0.181 mmol, 1 equiv.) in 15 ml of CH_2Cl_2 under

exclusion of light. The reaction mixture was stirred 1 h at room temperature, then it was filtered over Celite and concentrated under vacuum to *ca.* 0.5 ml of volume. The complex precipitated upon addition of *n*-pentane.

Yield: 79%, yellow solid.

- ^{1}H NMR: (500 MHz, $CDCl_3$, 25 °C): δ 1.13–1.44 (m, 9H, Cy), 1.52–1.95 (m, 13H, Cy), 2.05 (s, 6H, CH_3CN), 2.11–2.23 (br, 2H, CH_2PCy_2), 2.26–2.41 (br, 2H, CH_2PPh_2), 3.46–4.23 (br, 4H, CH_2 groups), 6.14 (m, 1H, C_6H_4), 6.87–6.99 (m, 1H, C_6H_4), 7.17–7.24 (m, 1H, C_6H_4), 7.29–7.34 (m, 1H, C_6H_4), 7.50–7.60 (m, 4H, Ph), 7.61–7.68 (m, 2H, Ph), 7.68–7.83 (m, 4H, Ph).
- ^{31}P{^{1}H} NMR: (202 MHz, $CDCl_3$, 25 °C): δ 26.9 (br, PPh_2), 50.4 (br, PCy_2).
- ^{19}F NMR: (188 MHz, $CDCl_3$, 25 °C): δ −78.7 (free triflate).
- Anal. Calcd. for $C_{38}H_{46}N_2O_6F_6P_2S_2Pd$ (973.28): C, 46.89; H, 4.76. Found: C, 47.01; H, 4.99.

5.5. X-ray crystallography

X-ray structures were measured on a Bruker CCD diffractometer (Bruker Smart Platform, with CCD detector, graphite monocromator, Mo Kα radiation). The program SMART served for the data collection. Integration was performed with SAINT. The structure solution and refinement on F^2 were accomplished with SHELXTL 97. Model plots were made with ORTEP32. All non-hydrogen atoms were refined freely with anisotropic displacements. The hydrogen atoms were refined at calculated positions riding on their carrier atoms. Weights are optimized in the final refinement cycles. Tables 8 and 9 give the crystallographic data for the compounds **2a** and [Pd(**1a**)(H_2O)(CH_3CN)](OTf)$_2$, respectively.

Table 8
Crystal data, measurement and refinement parameters for **2a**

Identification code	**2a**
Empirical formula	$C_{33}H_{42}Cl_4P_2Pd$
Formula weight	748.81
Temperature (K)	293(2)
Wavelength (Å)	0.71073
Crystal system	Monoclinic
Space group	$P2_1/c$
Unit cell dimensions	$a = 7.3814(15)$ Å $b = 19.374(4)$ Å $c = 24.251(5)$ Å $\alpha = 90°$ $\beta = 94.513(3)°$ $\gamma = 90°$
Volume (Å^3)	3457.4(12)
Z	4
Density (calc.) (mg cm^{-3})	1.439
Absorption coefficient (mm^{-1})	0.960
$F(0\,0\,0)$	1536
Crystal size (mm)	0.40 × 0.15 × 0.10
Theta range for data collection (°)	1.99–24.71
Limiting indices	$-8 \le h \le 8$, $-22 \le k \le 10$, $-28 \le l \le 28$
Reflections collected	16028
Independent reflections	5859 ($R_{int} = 0.0523$)
Completeness to theta	24.71°, 99.4%
Refinement method	Full-matrix least-squares on F^2
Data/restrains/parameters	5859/0/355
Goodness-of-fit on F^2	1.085
Final R indices [$I > 2$ sigma (I)]	$R1 = 0.0762$ $wR2 = 0.1971$
R indices (all data)	$R1 = 0.1069$ $wR2 = 0.2156$
Largest diff. peak and hole (e Å^{-3})	2.602, −1.850

Table 9
Crystal data, measurement and refinement parameters for **4a** (**4a** = [Pd(**1a**)(CH_3CN)(H_2O)](OTf)$_2$)

Identification code	**4a**
Empirical formula	$C_{37}H_{46}Cl_3F_6NO_7P_2PdS_2$
Formula weight	1069.56
Temperature (K)	293(2)
Wavelength (Å)	0.71073
Crystal system	Monoclinic
Space group	$P2_1/n$
Unit cell dimensions	$a = 11.9242(5)$ Å $b = 25.3192(12)$ Å $c = 15.0544(7)$ Å $\alpha = 90°$ $\beta = 97.0720(10)°$ $\gamma = 90°$
Volume (Å^3)	4510.5(4)
Z	4
Density (calc.) (mg cm^{-3})	1.575
Absorption coefficient (mm^{-1})	0.824
$F(0\,0\,0)$	2176
Crystal size (mm)	0.32 × 0.20 × 0.14
Theta range for data collection (°)	1.90–28.28
Limiting indices	$-14 \le h \le 15$, $-33 \le k \le 29$, $-20 \le l \le 12$
Reflections collected	33916
Independent reflections	11159 ($R_{int} = 0.0335$)
Completeness to theta	28.28°, 99.7%
Refinement method	Full-matrix least-squares on F^2
Data/restrains/parameters	11159/3/543
Goodness-of-fit on F^2	1.153
Final R indices [$I > 2$ sigma(I)]	$R1 = 0.0502$ $wR2 = 0.1083$
R indices (all data)	$R1 = 0.0588$ $wR2 = 0.1124$
Largest diff. peak and hole (e Å^{-3})	0.858, −0.583

5.6. Terpolymerization experiments

The copolymerization of carbon monoxide and propene was carried out in a 250 ml stainless steel autoclave (Nova Swiss). The pressure in the autoclave was measured with a manometer (Keller AG, range 0–400 bar) and with a piezoelectric sensor (range 0–400 bar). The autoclave employed for the catalytic test was charged with 273 mg (1.73 mmol) of 1,4-naphtoquinone, flushed three times with nitrogen and put under vacuum. 0.03 mmol of catalyst precursors **3a**–**d** were loaded into

a Schlenk tube under inert atmosphere and dissolved in 75 ml of THF "crown cap" and 4.5 ml of dry MeOH. The mixture was introduced in the autoclave by suction. The autoclave was then cooled to *ca.* −50 °C by means of a bath of acetone and dry ice. 19 g (0.45 mol) of propene were weighed and introduced in the cooled autoclave through a PVC tube. The autoclave was warmed up to room temperature and ethene was introduced by means of a Büchi pressflow controller 200. After pressurizing with 80 bar of carbon monoxide, the autoclave was heated up to 44 °C in a thermostat-regulated bath. The process was followed by monitoring the gas absoption in the autoclave. After 1.5–2 h the terpolymerization was interrupted. At the end of the reaction the autoclave was cooled down to room temperature and the non-reacted gases were released. The reaction mixture was concentrated and *ca.* 150 ml of MeOH were added to precipitate the copolymer. The copolymer was filtered off, washed with MeOH and dried under vacuum. The terpolymers were analyzed by means of NMR spectroscopy.

6. Supplementary material

Crystallographic data for the structural analysis have been deposited with the Cambridge Crystallographic Data Centre, CCDC nos. 281605 and 281608. These data can be obtained free of charge via www.ccdc.cam.ac.uk/data_request/cif, by e-mailing to data_request@ccdc.cam.ac.uk, or by contacting The Cambridge Crystallographic Data Centre, 12, Union Road, Cambridge CB2 1EZ, UK. Fax: +44 1223 336033.

Acknowledgment

We thank the Swiss National Science Foundation for the financial support.

Appendix A. Supplementary data

Supplementary data associated with this article can be found, in the online version, at doi:10.1016/j.molcata.2006.09.051.

References

[1] E. Drent, J.A.M. van Broekhoven, M.J. Doyle, J. Organomet. Chem. 417 (1991) 235.
[2] Z.Z. Jiang, S.E. Adams, A. Sen, Macromolecules 27 (1994) 2694.
[3] E.A. Klop, B.J. Lommerts, J. Veurink, J. Aerts, R.R. van Puijenbroek, J. Pol. Sci., B: Polym. Phys. 33 (1995) 315.
[4] F. Garbassi, A. Sommazzi, Polym. News 20 (1995) 201.
[5] A.S. Abu-Surrah, B. Rieger, Top. Catal. 7 (1999) 165.
[6] E. Drent, EP 121965 (1984).
[7] E. Drent, US patent 4,818,810 (1989).
[8] J.A. van Broekhoven, E. Drent, EP 0235865 (1987).
[9] J.A. van Broekhoven, E. Drent, E. Klei, EP 0213671 (1987).
[10] J.A. van Broekhoven, E. Drent, EP 0239145 (1987).
[11] S. Bronco, Diss. ETH no. 12043 (1997).
[12] B. Sesto, S. Bronco, E.L. Gindro, G. Consiglio, Macromol. Chem. Phys. 202 (2001) 2059.
[13] B. Sesto, Diss. ETH no. 14218 (2001).
[14] J.A. Davies, F.R. Hartley, Chem. Rev. 81 (1981) 79.
[15] W. Beck, Inorg. Synth. 28 (1990) 1.
[16] M. Sperrle, G. Consiglio, J. Am. Chem. Soc. 117 (1995) 12130.
[17] W.L. Steffen, G.J. Palenik, Inorg. Chem. 15 (1976) 2432.
[18] V.D. Makhaev, Z.M. Dzhabieva, S.V. Konovalikhin, O.A. Dyachenko, G.P. Belov, Koord. Khim. 22 (1996) 598.
[19] C. Gambs, G. Consiglio, A. Togni, Helv. Chim. Acta 84 (2001) 3105.
[20] W. Clegg, G.R. Eastham, M.R.J. Elsegood, B.T. Heaton, J.A. Iggo, R.P. Tooze, R. Whyman, S. Zacchini, Organometallics 21 (2002) 1832.
[21] A.J. Paviglianiti, D.J. Minn, W.C. Fultz, J.L. Burmeister, Inorg. Chim. Acta 159 (1989) 65.
[22] K.L. Li, P.N. Horton, M.B. Hursthouse, K.K. Hii, J. Organomet. Chem. 665 (2003) 250.
[23] J.M. Brown, K.K. Hii, Angew. Chem. Int. Ed. 35 (1996) 657.
[24] F. Ozawa, A. Kubo, Y. Matsumoto, T. Hayashi, E. Nishioka, K. Yanagi, K. Moriguchi, Organometallics 12 (1993) 4188.
[25] P.J. Stang, D.H. Cao, G.T. Poulter, A.M. Arif, Organometallics 14 (1995) 1110.
[26] F. Benetollo, R. Bertani, G. Bombieri, L. Toniolo, Inorg. Chim. Acta 233 (1995) 5.
[27] T. Hayashi, M. Konishi, Y. Kobori, M. Kumada, T. Higuchi, K. Hirotsu, J. Am. Chem. Soc. 106 (1984) 158.
[28] A. Leone, G. Consiglio, Helv. Chim. Acta 88 (2005) 210.
[29] A. Leone, Diss. ETH no. 16379 (2005).
[30] S. Bronco, G. Consiglio, R. Hutter, A. Batistini, U.W. Suter, Macromolecules 27 (1994) 4436.
[31] J.K.F. Buijink, E. Drent, J.C.L.J. Suiberbuyk, WO 0009583 (2000).
[32] A. Leone, S. Gischig, G. Consiglio, J. Organometal. Chem., in press.
[33] A. Leone, S. Gischig, C. J. Elsevier, G. Consiglio, submitted for publication.
[34] P. van Leeuwen, C.F. Roobeek, H. van der Heijden, J. Am. Chem. Soc. 116 (1994) 12117.
[35] G.K. Anderson, M. Lin, Inorg. Synth. 28 (1990) 60.